Bone Reports 12 (2020) 100258

Contents lists available at ScienceDirect

Bone Reports

journal homepage: www.elsevier.com/locate/bonr

RANKL-independent osteoclastogenesis in the SH3BP2 cherubism mice

Mizuho Kittaka[a,b], Tetsuya Yoshimoto[a,b], Henry Hoffman[c], Marcus Evan Levitan[a,b], Yasuyoshi Ueki[a,b,*]

[a] Department of Biomedical Sciences and Comprehensive Care, Indiana University, School of Dentistry, Indianapolis, IN 46202, USA
[b] Indiana Center for Musculoskeletal Health, Indiana University, School of Medicine, Indianapolis, IN 46202, USA
[c] Department of Oral and Craniofacial Sciences, University of Missouri-Kansas City, School of Dentistry, Kansas City, MO 64108, USA

ARTICLE INFO

Keywords:
RANKL-independent osteoclastogenesis
RANKL
SH3BP2
Cherubism
TNF-α

ABSTRACT

Even though the receptor activator of the nuclear factor-κB ligand (RANKL) and its receptor RANK have an exclusive role in osteoclastogenesis, the possibility of RANKL/RANK-independent osteoclastogenesis has been the subject of a long-standing debate in bone biology. In contrast, it has been reported that calvarial injection of TNF-α elicits significant osteoclastogenesis in the absence of RANKL/RANK in NF-κB2- and RBP-J-deficient mice, suggesting that inflammatory challenges and secondary gene manipulation are the prerequisites for RANKL/RANK-deficient mice to develop osteoclasts *in vivo*. Here we report that, even in the absence of RANKL ($Rankl^{-/-}$), cherubism mice ($Sh3bp2^{KI/KI}$) harboring the homozygous gain-of-function mutation in SH3-domain binding protein 2 (SH3BP2) develop tartrate-resistant acid phosphatase (TRAP)-positive multinucleated osteoclasts spontaneously. The $Sh3bp2^{KI/KI}$ $Rankl^{-/-}$ mice exhibit an increase in tooth exposure and a decrease in bone volume/total volume compared to $Sh3bp2^{+/+}$ $Rankl^{-/-}$ mice. The multinucleated cells were stained positively for cathepsin K. Osteoclastic marker gene expression in bone and serum TRAP5b levels were elevated in $Sh3bp2^{KI/KI}$ $Rankl^{-/-}$ mice. Elevation of the serum TNF-α levels suggested that TNF-α is a driver for the RANKL-independent osteoclast formation in $Sh3bp2^{KI/KI}$ mice. Our results provide a novel mutant model that develops osteoclasts independent of RANKL and establish that the gain-of-function of SH3BP2 promotes osteoclastogenesis not only in the presence of RANKL but also in the absence of RANKL.

1. Introduction

Osteoclasts are bone-degrading multinucleated cells critical for homeostatic bone remodeling and pathologic osteolysis (Novack, 2016). Histologically, the multinucleated cells are positive for tartrate-resistant acid phosphatase (TRAP) on the bone surfaces. Even though previous studies have established that the receptor activator of nuclear factor-κB ligand (RANKL) and its receptor RANK play a crucial role in osteoclast formation, RANKL/RANK-independent osteoclastogenesis in *in vivo* conditions of "wild-type mice" has been a long-standing debate (Tanaka, 2017). Recently, a study suggested the ability of wild-type osteoclast precursors to differentiate into functional osteoclasts *in vivo* in the absence of RANK (O'Brien et al., 2016). However, it is very difficult to exclude the possibility of incomplete deletion of the *Rank*, because inducible Mx1-Cre system was used to delete *Rankl* in the report (Okamoto et al., 2017). Instead, *in vivo* RANK/RANKL-independent osteoclastogenesis in a calvarial TNF-α injection model has been demonstrated in mice with deletion of signaling mediators such as NF-κB2 and RBP-J (Yao et al., 2009; Zhao et al., 2012).

Cherubism (OMIM#118400) is an autosomal-dominant craniofacial disorder in children characterized by expansive destruction of the maxilla and mandible. Gain-of-function mutations in the signaling adaptor SH3-domain binding protein 2 are responsible for the rare disorder (Ueki et al., 2001). We have shown that homozygous P416R knock-in (KI) mice ($Sh3bp2^{KI/KI}$) harboring the most common mutation in cherubism patients recapitulate the features of human cherubism by developing spontaneous fibrous inflammatory lesions and by exhibiting increased osteoclast formation in the jaw (Ueki et al., 2007). Heterozygous and homozygous cherubism mutations promote osteoclastogenesis induced by receptor activator of nuclear factor-κB ligand (RANKL) and tumor necrosis factor-alpha (TNF-α) (Ueki et al., 2007; Mukai et al., 2014).

Here, we show that homozygous $Sh3bp2^{KI/KI}$ mutant mice spontaneously develop TRAP-positive (+) multinucleated osteoclasts even when RANKL is absent. The $Sh3bp2^{KI/KI}$ $Rankl^{-/-}$ osteoclasts are also positive for cathepsin K. Reduced bone mass and increased levels of

* Corresponding author at: Indiana Center for Musculoskeletal Health, Indiana University School of Medicine, 635 Barnhill Dr., Van Nuys Medical Science Bldg. Room#514, Indianapolis, IN 46202, USA.
E-mail address: uekiy@iu.edu (Y. Ueki).

https://doi.org/10.1016/j.bonr.2020.100258
Received 17 February 2020; Accepted 16 March 2020
Available online 27 March 2020

serum markers for osteoclasts in *Sh3bp2*$^{KI/KI}$ *Rankl*$^{-/-}$ mice compared to *Sh3bp2*$^{+/+}$ *Rankl*$^{-/-}$ mice suggest that *Sh3bp2*$^{KI/KI}$ *Rankl*$^{-/-}$ osteoclasts are functionally active for bone resorption. Our data show that SH3BP2 has an *in vivo* regulatory role in promoting the differentiation cascade of osteoclast progenitors to mature osteoclasts not only in the presence of RANKL but also in the absence of RANKL. Also, the *Sh3bp2*$^{KI/KI}$ *Rankl*$^{-/-}$ mice provide a new piece of evidence that genetic manipulation is necessary for developing functional osteoclasts in the absence of RANK/RANKL.

2. Materials and methods

2.1. Mice

All animal experiments in this study were performed according to protocols approved by the IACUCs of the University of Missouri-Kansas City and Indiana University. *Sh3bp2*$^{KI/KI}$ mice have been created previously (Ueki et al., 2007). RANKL-deficient (*Rankl*$^{-/-}$) mice were created by crossing *Rankl*$^{fl/fl}$ mice with *EIIa-Cre* mice. *Rankl*$^{fl/fl}$ (#018978) and *EIIa-Cre* (#003724) mice were obtained from the Jackson laboratory (Bar Harbor, ME, USA). All mice were crossed and created on the mix background of C57BL/6 and 129 × 1/SvJ under specific pathogen-free conditions and analyzed at 20 weeks old.

2.2. Ex-vivo microCT (μCT) analysis

Jaw bone and femur from 20-week old mice were fixed with 4% paraformaldehyde (PFA) in PBS for 24 h and soaked in 70% ethanol for scanning with the Skyscan 1174 (Bruker, Kontich, Belgium). Scanning conditions are as follows: 80 kV X-ray energy, 6.67 μm pixel size, and 0.4° rotation step with 3000 ms of exposure time. Scanned data were reconstructed with NRecon software (Bruker) with 0 to 0.16 of dynamic range. 3D images were created using CTVox software (Bruker) based on volume rendering method. Reconstructed data were aligned using Dataviewer software (Bruker). The % of exposed tooth width was measured using the midpoint of the lower 3rd molar. Femur length and bone volume/tissue volume of trabecular bone (within one-fourth length of the femur from the middle point toward the distal end) were measured with the CTAnalyzer software (Bruker).

2.3. Histology

After μCT analysis, mandible and femur were decalcified with EDTA (0.5 M, pH 7.2) and embedded in paraffin. Six μm sections were subjected to hematoxylin and eosin (H&E) and TRAP staining, and immunohistochemistry for Cathepsin K. Images were captured using the BZ-X800 microscope (Keyence, Osaka, Japan).

2.4. Histomorphometry of TRAP-positive osteoclasts

The number of TRAP + cells underneath the growth plate of the distal end of the femur was measured by Bioquant (Bioguant Image Analysis Corporation, Nashville, TN). Trabecular bone within 3 mm underneath the growth plate was separated into three regions (1 mm each) and the number of TRAP + cells was counted in each region of interest (ROI). Two sections separated by at least 30 μm were analyzed for each mouse and the numbers were averaged.

2.5. Immunohistochemical staining

Tissue sections were deparaffinized and rehydrated, then endogenous peroxidase was blocked with 3% H_2O_2/PBS solution. After blocking with 2% goat serum, sections were incubated with an antibody against Cathepsin K (ab19027, Abcam) overnight at 4 °C. After washing with PBS, sections were incubated with biotinylated goat secondary antibody (Vector Laboratories, Burlingame, CA, USA) for 60 min at room temperature followed by treatment with Vectastain elite ABC kit (Vector Laboratories). Sections were colored using ImmPACT DAB (Vector Laboratories) and counterstained with hematoxylin.

2.6. RNA extraction from femurs

After removing soft tissues, head and distal end of the femur were cut off. The remaining part of the femur was flash frozen in liquid nitrogen and crushed in powder using a tissue pulverizer (Cellcrusher Limited, Schull, Ireland) for RNA isolation (Ribozol, VWR, Radnor, PA, USA).

2.7. Reverse transcription-quantitative PCR (RT-qPCR)

Five hundred nanograms of total RNA was transcribed to cDNA using the High Capacity cDNA Reverse Transcription Kit (Life Technologies, Carlsbad, CA, USA). qPCR reactions were performed with the StepOne Plus System (Life Technologies) using Maxima SYBR green mix (Thermo Fisher Scientific, Waltham, MA, USA). qPCR primers published in our previous study were used in this study (Kittaka et al., 2020). Relative gene expression levels were calculated using a relative-standard curve method. All gene expression levels were normalized by the expression level of *Hprt*.

2.8. Serum ELISA

Mouse TNF-α Duo-Set ELISA kit (R&D Systems, Minneapolis, MN, USA), mouse TRAP5b assay kit (Immunodiagnostic Systems, Boldon, UK), and RatLaps CTX-I EIA kit (Immunodiagnostic Systems) were used to measure serum levels of TNF-α, TRAP5b, and CTX. Serum was separated from blood with Vacutainer collection tube (BD, Franklin Lakes, NJ, USA) and stored at −80 °C until use.

2.9. Statistics

The two-tailed unpaired Student's *t*-test was used to compare two groups. One-way ANOVA with Tukey-Kramer *post hoc* test was used to compare three or more groups. GraphPad Prism (ver. 8, GraphPad Software, La Jolla, CA, USA) was used for all statistical analyses. The p values < 0.05 were considered significant.

3. Results

3.1. Homozygous gain-of-function mutation in SH3BP2 improves osteopetrosis in RANKL-deficient mice

We have previously reported that the gain-of-function mutation in SH3BP2 (*Sh3bp2*$^{KI/KI}$), which is responsible for cherubism, increases the susceptibility of bone marrow-derived M-CSF-dependent macrophages (BMMs) to TNF-α and stimulates the osteoclast formation independent of RANKL *in vitro* (Mukai et al., 2014). Therefore, we hypothesized that the *Sh3bp2*$^{KI/KI}$ mutation may improve osteopetrosis in RANKL-deficient (*Rankl*$^{-/-}$) mice by inducing osteoclasts.

To test this hypothesis, we created *Sh3bp2*$^{KI/KI}$ *Rankl*$^{-/-}$ double mutant mice. MicroCT analysis found that while the *Sh3bp2*$^{KI/KI}$ mutation fails to exhibit tooth eruption (Fig. 1A), alveolar bone covering the tooth is significantly less than *Rankl*$^{-/-}$ mice (Fig. 1B). The *Sh3bp2*$^{KI/KI}$ mutation increased the femur length in males, but improved osteopetrosis by decreasing bone volume/total volume (BV/TV) at distal femur in male and female *Rankl*$^{-/-}$ mice (Fig. 1C, D). The smaller bodyweight of *Rankl*$^{-/-}$ mice was not restored by the *Sh3bp2*$^{KI/KI}$ mutation (Fig. 1E). H&E staining confirmed that the route for tooth eruption is open more widely and that bone marrow spaces occupied by hematopoietic cells are more expanded in *Sh3bp2*$^{KI/KI}$ *Rankl*$^{-/-}$ mice than *Rankl*$^{-/-}$ mice (Fig. 1F, G). These data present that the *Sh3bp2*$^{KI/KI}$ mutation improves the osteopetrotic phenotype of

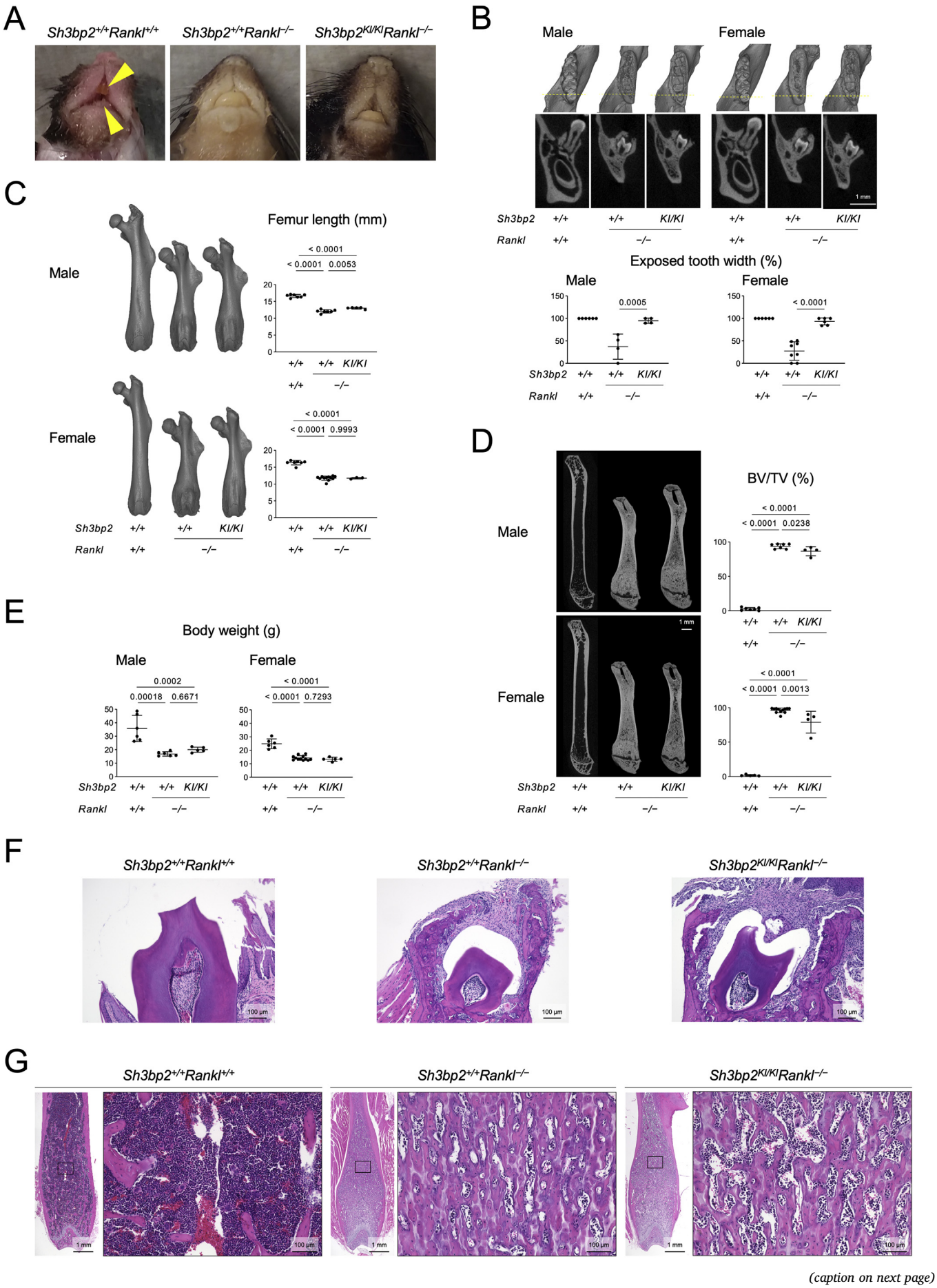

(caption on next page)

Fig. 1. (A) Representative images showing incisor eruption. Arrowheads indicate erupted incisors in the wild-type mouse at 20 weeks old. (B) Left top: 3D μCT images of the mandibular molars. Left bottom: 2D coronal μCT images at the yellow line. Right: Percentage of opening width of the tooth measured at the midpoints of the lower third molar. (C) Left: 3D μCT images of the femur. Right: length of the femur. (D) Left: 2D sagittal μCT images of the femur. Right: Bone volume (BV)/tissue volume (TV) of trabecular bone. (E) Body weight of the mice. (F) H&E staining of the mandibular third molar. Bar = 100 μm. (G) H&E staining of the femur. Boxes represent the area shown at higher magnification. Mice were analyzed at 20 weeks old. All images are representative from male mice. Data are mean ± SD. Each dot in graphs represent a value from a single biological sample. *p* values in graphs were calculated by one-way ANOVA with Tukey's multiple comparison test. $p < 0.05$ was considered to be significantly different.

Rankl$^{-/-}$ mice.

3.2. RANKL-deficient *Sh3bp2*$^{KI/KI}$ mice develop TRAP+ osteoclasts

To examine whether *Sh3bp2*$^{KI/KI}$ *Rankl*$^{-/-}$ mice develop osteoclasts *in vivo*, we performed TRAP staining on alveolar and trabecular bone sections from the mandible and femur of the *Sh3bp2*$^{KI/KI}$ *Rankl*$^{-/-}$ mice. Although the overall TRAP-positive (+) osteoclast number was much smaller than *Sh3bp2*$^{+/+}$ *Rankl*$^{+/+}$ mice, a number of TRAP+ multinucleated osteoclasts were developed on the bone surface of *Sh3bp2*$^{KI/KI}$ *Rankl*$^{-/-}$ mice (Fig. 2A, B). The number was increased toward the growth plate in male *Sh3bp2*$^{KI/KI}$ *Rankl*$^{-/-}$ mice (Fig. 2C). The TRAP+ multinucleated cells were stained positively for an osteoclast marker cathepsin K (Fig. 2D). Consistent with the presence of TRAP+ and cathepsin K+ cells, expression levels of osteoclast marker genes such as *Acp5*, *Cathepsin K*, and *Mmp9* were increased in the femur of *Sh3bp2*$^{KI/KI}$ *Rankl*$^{-/-}$ mice compared to *Sh3bp2*$^{+/+}$ *Rankl*$^{-/-}$ mice (Fig. 2E). Serum TRAP5b levels were elevated in *Sh3bp2*$^{KI/KI}$ *Rankl*$^{-/-}$ mice and serum CTX levels were increased in female *Sh3bp2*$^{KI/KI}$ *Rankl*$^{-/-}$ mice compared to *Sh3bp2*$^{+/+}$ *Rankl*$^{-/-}$ mice (Fig. 2F). Consistent with our previous results, *Sh3bp2*$^{KI/KI}$ mutation increased serum TNF-α levels in *Rankl*$^{-/-}$ mice (Fig. 2G). In contrast, RANKL deletion suppressed the elevation of serum TNF-α in *Sh3bp2*$^{KI/KI}$ cherubism mice (Fig. 2G). Together, the data suggest that *Sh3bp2*$^{KI/KI}$ *Rankl*$^{-/-}$ osteoclasts are functionally active and that TNF-α substitutes for RANKL to develop TRAP+ osteoclasts in *Sh3bp2*$^{KI/KI}$ *Rankl*$^{-/-}$ mice.

4. Discussion

We have previously shown that bone marrow-derived M-CSF-dependent macrophages harboring a gain-of-function mutation in SH3BP2 are highly susceptible to TNF-α, and they can form TRAP+ osteoclasts independent of RANKL *in vitro* (Mukai et al., 2014). In this study, we showed that the *Sh3bp2*$^{KI/KI}$ mutation can develop TRAP+ multinucleated osteoclasts in RANKL-deficient mice spontaneously. It also improved the osteopetrotic phenotype of the mice, presumably cooperated with impaired osteoblast function of *Sh3bp2*$^{KI/KI}$ mice (Mukherjee et al., 2010; Wang et al., 2010).

To our best knowledge, RANKL-deficient *Sh3bp2*$^{KI/KI}$ mice are the third model that develops RANK/RANKL-independent osteoclasts after the *NFkb2*$^{-/-}$ and *Rbpj*$^{\Delta M/\Delta M}$ mice injected with TNF-α on the calvaria (Yao et al., 2009; Zhao et al., 2012). However, they are the first human disease model that exhibits RANK/RANKL-independent osteoclastogenesis. Also, *Sh3bp2*$^{KI/KI}$ *Rankl*$^{-/-}$ mice are the second model that shows the spontaneous osteoclast development in the absence of the RANK/RANKL signaling following the *Rbpj*$^{\Delta M/\Delta M}$ mice, although Zhao et al. did not clarify whether TRAP+ cells in the calvaria of PBS-injected *Rank*$^{-/-}$ *Rbpj*$^{\Delta M/\Delta M}$ mice are osteoclasts or not (in the Fig. 3F of (Zhao et al., 2012)).

Even though the possibility of RANKL/RANK-independent osteoclastogenesis in wild-type mice has been a long-standing debate, many cell culture studies have suggested the RANK/RANKL-independent osteoclastogenesis of wild-type osteoclast precursors (Tanaka, 2017; Okamoto et al., 2017). Notably, Kim et al. showed that M-CSF/TGF-β-dependent osteoclast precursors from RANKL- and RANK-deficient mice are able to form functionally active osteoclasts when stimulated with TNF-α and IL-1 (IL-1 types are not specified in the report) (Kim et al., 2005). However, the consequences of TNF-α and IL-1 stimulation *in vivo* were not explored in this study.

A recent study by O'Brien et al. showed TRAP+ osteoclast formation in the K/BxN serum-transfer arthritis model, in which RANK is deleted by *Mx1-Cre* (O'Brien et al., 2016). However, it is difficult to exclude the possibility of incomplete deletion of the *Rank* gene, because *Cre* is inducibly expressed in type I interferon receptor (IFNAR)-expressing cells after polyinosine-polycytidylic acid (pIpC) injection (Okamoto et al., 2017; Kuhn et al., 1995). Therefore, the current consensus on RANK/RANKL-independent osteoclastogenesis is that additional gene manipulation is required for RANK/RANKL-deficient mice to develop osteoclasts *in vivo*. Because *Sh3bp2*$^{KI/KI}$ *Rankl*$^{-/-}$ mice show not only a decrease in BV/TV but also an increase in bone resorption markers in serum compared to *Sh3bp2*$^{+/+}$ *Rankl*$^{-/-}$ mice, homozygous *Sh3bp2*$^{KI/KI}$ mutation serves as a new genetic manipulation to enable the formation of functional osteoclasts in the absence of RANKL.

We have previously shown that retroviral overexpression of wild-type and cherubism mutant form of SH3BP2 in RAW264.7 cells induces TRAP+ multinucleated cells without RANKL stimulation (Levaot et al., 2011). We have also shown that TNF-α stimulation in the presence of SH3BP2 gain-of-function can induce osteoclastogenesis *via* the SYK-NFATc1 axis (Mukai et al., 2014). These results suggest that activation of the downstream signaling of SH3BP2 play a crucial role in RANKL-independent osteoclast formation. Since the gain-of-function of SH3BP2 increases SYK activation in myeloid cells (Ueki et al., 2007; Mukai et al., 2014; Yoshitaka et al., 2014), SYK is likely involved in the mechanism of RANKL-independent osteoclastogenesis. Pathological conditions caused by the hyperactivation of SYK in myeloid lineage cells (Puissant et al., 2014; Mocsai et al., 2010; Ozaki et al., 2012) may exhibit bone loss independent of RANKL, at least in part. Individuals with loss-of-function mutations in RANK or RANKL exhibit osteopetrosis (Guerrini et al., 2008; Sobacchi et al., 2007). Because tankyrase inhibitors can activate the SH3BP2-SYK pathway in osteoclasts by preventing SH3BP2 protein from degradation (Fujita et al., 2018), patients with certain types of osteopetrosis may benefit from tankyrase inhibitor treatment by inducing RANK/RANKL-independent osteoclastic bone resorption.

Elevation of the serum CTX in *Sh3bp2*$^{KI/KI}$ *Rankl*$^{-/-}$ mice was significant in females, but not in males. The gender-dependent effect may be explained by the possibility that not all *Sh3bp2*$^{KI/KI}$ *Rankl*$^{-/-}$ TRAP+ cells have active bone resorption capacity in males. In addition, a supplemental analysis revealed that male *Sh3bp2*$^{KI/KI}$ *Rankl*$^{-/-}$ mice show the increase in serum CTX ($p < 0.01$) if an outlier is excluded in each group (Grubbs' method with $\alpha = 0.05$).

Intriguingly, lack of RANKL decreased the serum TNF-α elevation in *Sh3bp2*$^{KI/KI}$ cherubism mice. This result suggests that the RANK-mediated signaling in macrophages plays a critical role in the development or exacerbation of autoinflammation in cherubism mice. Together, RANKL inhibitors might be beneficial for suppressing the development of lesions in cherubism patients. These hypotheses need to be validated in further studies.

In conclusion, we showed that the cherubism mice carrying the gain-of-function mutation in SH3BP2 develop osteoclasts in a RANKL-independent manner. These results will reinforce our current understanding that SH3BP2 is an adaptor protein critical for the regulation of osteoclastogenesis and that additional gene manipulation is necessary

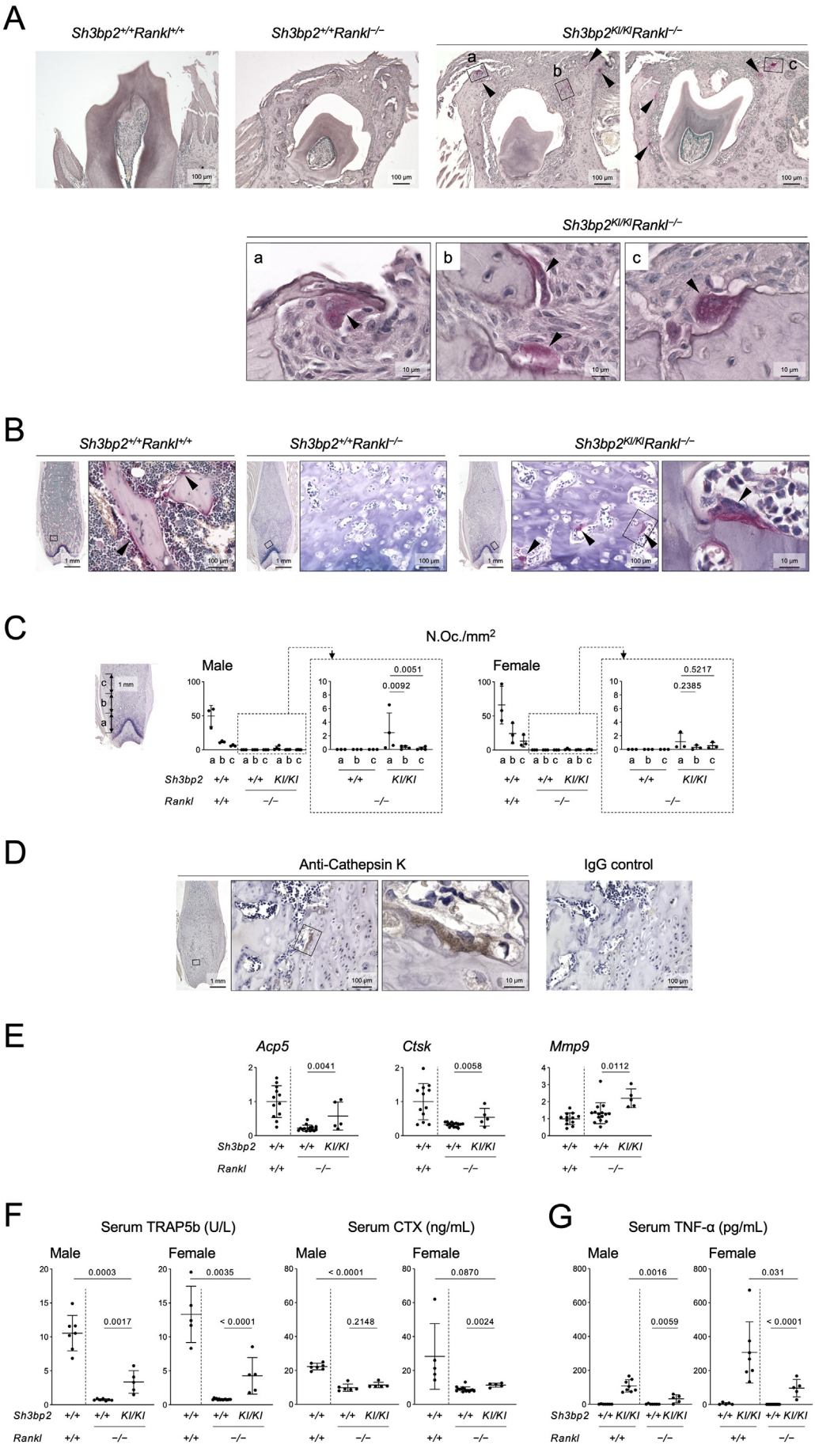

Fig. 2. (A) TRAP staining of alveolar bone surrounding the mandibular third molar. The boxes represent the area shown at higher magnification. Arrowheads indicate TRAP + cells on the bone surface. (B) TRAP staining of trabecular bone of the femur. Boxes represent the area shown at higher magnification. Arrowheads indicate TRAP + cells on the bone surface. (C). Left: An image showing the ROI. Middle: The number of TRAP + osteoclasts/mm^2 in each ROI (a, b, c). Right: The number of TRAP + osteoclasts/mm^2 from *Rankl*$^{-/-}$ mice. (D) Immunohistochemistry of cathepsin K. Boxes represent the area shown at higher magnification. (E) qPCR analysis of osteoclast maker gene expression in the femur. Average expression levels in the wild-type mice were set as 1. (F) Serum levels of TRAP5b and CTX. (G) Serum levels of TNF-α. Mice were analyzed at 20 weeks old. All images are representative from male mice. Data are mean ± SD. Each dot in graphs represents a value from a single biological sample. p values in graphs were calculated by one-way ANOVA with Tukey's multiple comparison test (C) or t-test (E, F, G). $p < 0.05$ was considered to be significantly different.

for achieving osteoclastogenesis in the absence of RANK/RANKL.

Authors' contribution

MK and YU conceived the idea and initiated the project. MK generated the mice. MK, TY, HH, and MEL conducted analyses and contributed to the data interpretation. YU wrote the manuscript, and all authors approved the final version of the manuscript. MK and YU take responsibility for the integrity of the data and analysis.

Funding

This work was supported by the National Institutes of Health (R01DE025870 and R21AR070953 to YU). The content is solely the responsibility of the authors and does not necessarily represent the official views of the NIH.

Declaration of competing interest

The authors have no conflict of interest to declare.

Acknowledgements

MK is a recipient of a fellowship from the Brain Circulation Program to develop new leaders for international dental education course through international collaborative dental research, Japan, and of a fund for young researchers from Japanese Society of Periodontology. TY is a recipient of the Japan Society for the Promotion of Science (JSPS) Overseas Research Fellowship. We appreciate Tianli Zhu at the Indiana University School of Dentistry for technical assistance for histology. The authors declare no conflicts of interest.

References

Fujita, S., Mukai, T., Mito, T., Kodama, S., Nagasu, A., Kittaka, M., Sone, T., Ueki, Y., Morita, Y., 2018. Pharmacological inhibition of tankyrase induces bone loss in mice by increasing osteoclastogenesis. Bone 106, 156–166.

Guerrini, M.M., Sobacchi, C., Cassani, B., Abinun, M., Kilic, S.S., Pangrazio, A., Moratto, D., Mazzolari, E., Clayton-Smith, J., Orchard, P., Coxon, F.P., Helfrich, M.H., Crockett, J.C., Mellis, D., Vellodi, A., Tezcan, I., Notarangelo, L.D., Rogers, M.J., Vezzoni, P., Villa, A., Frattini, A., 2008. Human osteoclast-poor osteopetrosis with hypogammaglobulinemia due to TNFRSF11A (RANK) mutations. Am. J. Hum. Genet. 83, 64–76.

Kim, N., Kadono, Y., Takami, M., Lee, J., Lee, S.H., Okada, F., Kim, J.H., Kobayashi, T., Odgren, P.R., Nakano, H., Yeh, W.C., Lee, S.K., Lorenzo, J.A., Choi, Y., 2005. Osteoclast differentiation independent of the TRANCE-RANK-TRAF6 axis. J. Exp. Med. 202, 589–595.

Kittaka, M., Yoshimoto, T., Schlosser, C., Rottapel, R., Kajiya, M., Kurihara, H., Reichenberger, E.J., Ueki, Y., 2020. Alveolar bone protection by targeting the SH3BP2-SYK axis in osteoclasts. J. Bone Miner. Res. 35, 382–395.

Kuhn, R., Schwenk, F., Aguet, M., Rajewsky, K., 1995. Inducible gene targeting in mice. Science 269, 1427–1429.

Levaot, N., Voytyuk, O., Dimitriou, I., Sircoulomb, F., Chandrakumar, A., Deckert, M., Krzyzanowski, P.M., Scotter, A., Gu, S., Janmohamed, S., Cong, F., Simoncic, P.D., Ueki, Y., La Rose, J., Rottapel, R., 2011. Loss of Tankyrase-mediated destruction of 3BP2 is the underlying pathogenic mechanism of cherubism. Cell 147, 1324–1339.

Mocsai, A., Ruland, J., Tybulewicz, V.L., 2010. The SYK tyrosine kinase: a crucial player in diverse biological functions. Nat Rev Immunol 10, 387–402.

Mukai, T., Ishida, S., Ishikawa, R., Yoshitaka, T., Kittaka, M., Gallant, R., Lin, Y.L., Rottapel, R., Brotto, M., Reichenberger, E.J., Ueki, Y., 2014. SH3BP2 cherubism mutation potentiates TNF-alpha-induced osteoclastogenesis via NFATc1 and TNF-alpha-mediated inflammatory bone loss. J. Bone Miner. Res. 29, 2618–2635.

Mukherjee, P.M., Wang, C.J., Chen, I.P., Jafarov, T., Olsen, B.R., Ueki, Y., Reichenberger, E.J., 2010. Cherubism gene Sh3bp2 is important for optimal bone formation, osteoblast differentiation, and function. Am. J. Orthod. Dentofac. Orthop. 138 (140 e1-140 e11; discussion 140-1).

Novack, D.V., 2016. Editorial: inflammatory osteoclasts: a different breed of bone eaters? Arthritis Rheumatol. 68, 2834–2836.

O'Brien, W., Fissel, B.M., Maeda, Y., Yan, J., Ge, X., Gravallese, E.M., Aliprantis, A.O., Charles, J.F., 2016. RANK-independent osteoclast formation and bone erosion in inflammatory arthritis. Arthritis Rheumatol 68, 2889–2900.

Okamoto, K., Nakashima, T., Shinohara, M., Negishi-Koga, T., Komatsu, N., Terashima, A., Sawa, S., Nitta, T., Takayanagi, H., 2017. Osteoimmunology: the conceptual framework unifying the immune and skeletal systems. Physiol. Rev. 97, 1295–1349.

Ozaki, N., Suzuki, S., Ishida, M., Harada, Y., Tanaka, K., Sato, Y., Kono, T., Kubo, M., Kitamura, D., Encinas, J., Hara, H., Yoshida, H., 2012. Syk-dependent signaling pathways in neutrophils and macrophages are indispensable in the pathogenesis of anti-collagen antibody-induced arthritis. Int. Immunol. 24, 539–550.

Puissant, A., Fenouille, N., Alexe, G., Pikman, Y., Bassil, C.F., Mehta, S., Du, J., Kazi, J.U., Luciano, F., Ronnstrand, L., Kung, A.L., Aster, J.C., Galinsky, I., Stone, R.M., DeAngelo, D.J., Hemann, M.T., Stegmaier, K., 2014. SYK is a critical regulator of FLT3 in acute myeloid leukemia. Cancer Cell 25, 226–242.

Sobacchi, C., Frattini, A., Guerrini, M.M., Abinun, M., Pangrazio, A., Susani, L., Bredius, R., Mancini, G., Cant, A., Bishop, N., Grabowski, P., Del Fattore, A., Messina, C., Errigo, G., Coxon, F.P., Scott, D.I., Teti, A., Rogers, M.J., Vezzoni, P., Villa, A., Helfrich, M.H., 2007. Osteoclast-poor human osteopetrosis due to mutations in the gene encoding RANKL. Nat. Genet. 39, 960–962.

Tanaka, S., 2017. RANKL-independent osteoclastogenesis: a long-standing controversy. J. Bone Miner. Res. 32, 431–433.

Ueki, Y., Tiziani, V., Santanna, C., Fukai, N., Maulik, C., Garfinkle, J., Ninomiya, C., do Amaral, C., Peters, H., Habal, M., Rhee-Morris, L., Doss, J.B., Kreiborg, S., Olsen, B.R., Reichenberger, E., 2001. Mutations in the gene encoding c-Abl-binding protein SH3BP2 cause cherubism. Nat. Genet. 28, 125–126.

Ueki, Y., Lin, C.Y., Senoo, M., Ebihara, T., Agata, N., Onji, M., Saheki, Y., Kawai, T., Mukherjee, P.M., Reichenberger, E., Olsen, B.R., 2007. Increased myeloid cell responses to M-CSF and RANKL cause bone loss and inflammation in SH3BP2 "cherubism" mice. Cell 128, 71–83.

Wang, C.J., Chen, I.P., Koczon-Jaremko, B., Boskey, A.L., Ueki, Y., Kuhn, L., Reichenberger, E.J., 2010. Pro416Arg cherubism mutation in Sh3bp2 knock-in mice affects osteoblasts and alters bone mineral and matrix properties. Bone 46, 1306–1315.

Yao, Z., Xing, L., Boyce, B.F., 2009. NF-kappa B p 100 limits TNF-induced bone resorption in mice by a TRAF3-dependent mechanism. J. Clin. Invest. 119, 3024–3034.

Yoshitaka, T., Mukai, T., Kittaka, M., Alford, L.M., Masrani, S., Ishida, S., Yamaguchi, K., Yamada, M., Mizuno, N., Olsen, B.R., Reichenberger, E.J., Ueki, Y., 2014. Enhanced TLR-MYD88 signaling stimulates autoinflammation in SH3BP2 cherubism mice and defines the etiology of cherubism. Cell Rep. 8, 1752–1766.

Zhao, B., Grimes, S.N., Li, S., Hu, X., Ivashkiv, L.B., 2012. TNF-induced osteoclastogenesis and inflammatory bone resorption are inhibited by transcription factor RBP-J. J. Exp. Med. 209, 319–334.